J|A|C|S
ARTICLES
Published on Web 09/06/2006

Elasticity of Crystalline β-Sheet Monolayers

Hila Isenberg,[†] Kristian Kjaer,[‡] and Hanna Rapaport*,[†]

Contribution from the Department of Biotechnology Engineering, Ben-Gurion University of the Negev, Beer-Sheva 84105, Israel, and Niels Bohr Institute, University of Copenhagen, DK-2100 Copenhagen, Denmark

Received April 14, 2006; Revised Manuscript Received July 30, 2006; E-mail: hannarap@bgu.ac.il

Abstract: Designed amphiphilic β-sheet peptides with the sequence Pro−Glu−(Phe−Glu)$_n$−Pro ($n = 2-7$) were previously shown by grazing incidence X-ray diffraction (GIXD), to form ordered two-dimensional (2-D) monolayer structures at interfaces induced by the proline residues at peptide termini. The GIXD diffraction pattern was modeled with two coexisting lattice arrangements, suggesting structural flexibility exhibited in the multiple ways by which β-strands and their amino acid side chains pack into ordered 2-D structures. Here, we find by in-situ GIXD measurements that the ordered β-sheet assemblies may undergo a quasi-reversible compression and expansion cycle at the air−water interface. The diffraction measurements indicate that on compression the repeat distance that corresponds to the long axes of the peptide strands may decrease by up to 37% in length. Upon expansion the compressed β-sheet assemblies revert elastically to their original conformation. The interstrand repeat distance along the peptide hydrogen bonds apparently does not change along the film compression and expansion. Based on the GIXD data, at surface pressures higher than ~3 mN/m, beyond the peptide limiting area per molecule, the compressibility is 7.4 ± 0.6 m/N. The out-of-plane Bragg rod diffraction patterns imply that in the compressed state the β-strands buckle up in reaction to the increase in surface pressure. At low surface pressure, the 2-D compressibility of the crystalline β-sheet was estimated at ~32 m/N attributed to interdomain rearrangements.

Introduction

Molecular systems composed of designed peptides or proteins can be programmed to yield intriguing and potentially useful supramolecular architectures. In the search for advanced biomaterials with predictable properties, there has been growing interest in amphiphilic peptide self-assembly architectures. Amphiphilic peptides, which display hydrophobic and hydrophilic amino acids, may induce particular folds that are sequence dependent. Novel biomaterials composed of amphiphilic β-sheet molecular assemblies have been engineered in a bottom to top approach to form a variety of supramolecular architectures.[1−8] The β-sheet structure is composed of pleated β-strands that are stabilized by interstrand hydrogen bonds and by intermolecular interactions between amino acids side chains. Recently, it has been shown that rationally designed peptides may form ordered β-sheet monolayers at flat solid surfaces and at air−aqueous solution interfaces.[5,9−12] Ordered amphiphilic peptide monolayers at interfaces may provide planar scaffolds relevant to a broad spectrum of nanometer-scale applications. By combining self-assembled molecular systems with current lithography techniques,[13] sophisticated molecular architectures may be developed. Advanced understanding of peptide assemblies at the molecular level would enable further utilization of such systems in applications that require nanometer-scale precision.

Detailed structural characterization of a group of amphiphilic peptides, Pro−Glu−(Phe−Glu)$_n$−Pro, denoted by P_{Glu}-*n*, which form β-sheet monolayers at air−water solution interfaces, has been provided by in-situ grazing incidence X-ray diffraction (GIXD) measurements.[11] The alternating hydrophilic (Glu) and hydrophobic (Phe) amino acids along the peptide backbone induce the β-strand conformation at air−water interfaces. Phe was selected as the hydrophobic amino acid for its relatively large side chain that is advantageous in X-ray diffraction measurements. Phe side chains may also form favorable phenyl−phenyl interactions between neighboring strands.[14] The

[†] Ben-Gurion University of the Negev.
[‡] University of Copenhagen.

(1) Aggeli, A.; Nyrkova, I. A.; Bell, M.; Harding, R.; Carrick, L.; McLeish, T. C. B.; Semenov, A. N.; Boden, N. *Proc. Natl. Acad. Sci. U.S.A.* **2001**, *98*, 11857−11862.
(2) Bong, D. T.; Clark, T. D.; Granja, J. R.; Ghadiri, M. R. *Angew. Chem., Int. Ed.* **2001**, *40*, 988−1011.
(3) Smeenk, J. M.; Otten, M. B. J.; Thies, J.; Tirrell, D. A.; Stunnenberg, H. G.; van Hest, J. C. M. *Angew. Chem., Int. Ed.* **2005**, *44*, 1968−1971.
(4) Zhang, S. G.; Holmes, T.; Lockshin, C.; Rich, A. *Proc. Natl. Acad. Sci. U.S.A.* **1993**, *90*, 3334−3338.
(5) Xu, G.; Wang, W.; Groves, J. T.; Hecht, M. H. *Proc. Natl. Acad. Sci. U.S.A.* **2001**, *98*, 3652−3657.
(6) Powers, E. T.; Yang, S. I.; Lieber, C. M.; Kelly, J. W. *Angew. Chem., Int. Ed.* **2002**, *41*, 127−130.
(7) Sneer, R.; Weygand, M. J.; Kjaer, K.; Tirrell, D. A.; Rapaport, H. *Chem. Phys. Chem.* **2004**, *5*, 747−750.
(8) Rapaport, H.; Kjaer, K.; Jensen, T. R.; Moller, G.; Knobler, C.; Leiserowitz, L.; Tirrell, D. A. *J. Am. Chem. Soc.* **2002**, *124*, 9342−9343.
(9) Bekele, H.; Fendler, J. H.; Kelly, J. W. *J. Am. Chem. Soc.* **1999**, *121*, 7266−7267.
(10) Whitehouse, C.; Fang, J.; Aggeli, A.; Bell, M.; Brydson, R.; Fishwick, C. W. G.; Henderson, J. R.; Knobler, C. M.; Owens, R. W.; Thomson, N. H.; Alastair Smith, D.; Boden, N. *Angew. Chem., Int. Ed.* **2005**, *44*, 1965−1968.
(11) Rapaport, H.; Kjaer, K.; Jensen, T. R.; Leiserowitz, L.; Tirrell, D. A. *J. Am. Chem. Soc.* **2000**, *122*, 12523−12529.
(12) Rapaport, H. *Supramol. Chem.* **2006**, *18*, 445−454.
(13) Zhang, S. G.; Yan, L.; Altman, M.; Lassle, M.; Nugent, H.; Frankel, F.; Lauffenburger, D. A.; Whitesides, G. M.; Rich, A. *Biomaterials* **1999**, *20*, 1213−1220.

10.1021/ja062363q CCC: $33.50

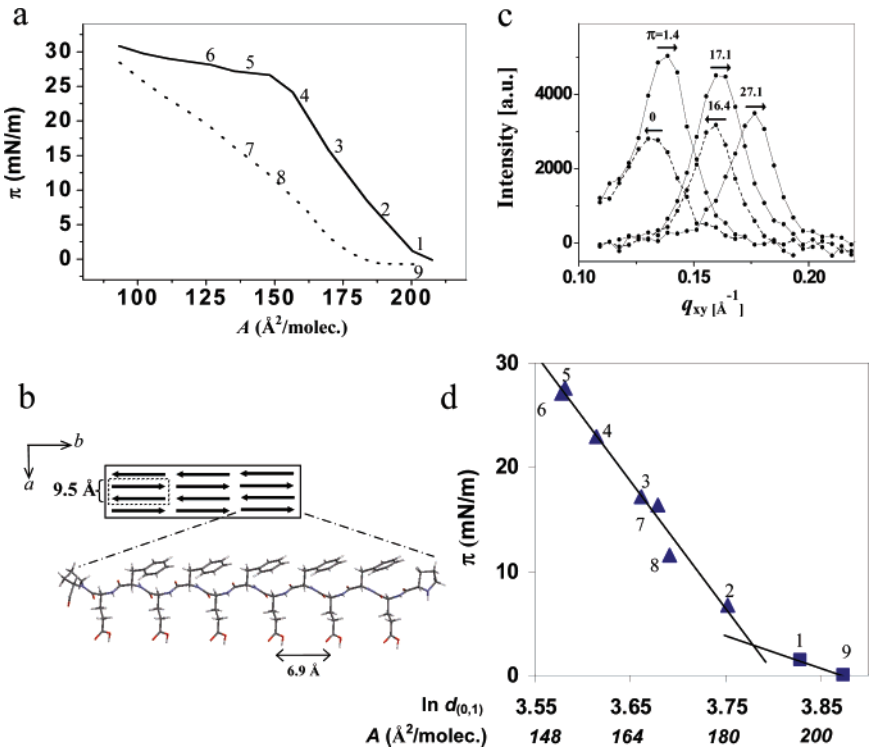

Figure 1. (a) Surface pressure versus mean molecular area isotherm of P_{Glu}-5 showing the compression (−) and expansion (- - -) of the film. These curves represent the general trend of the isotherm measured during the GIXD studies. The latter isotherm (which is provided in the Supporting Information) exhibits drops in surface pressure, due to relaxation, a commonly observed behavior of Langmuir films, at points where film compression is halted to allow GIXD measurements (these points that correspond to the states where GIXD measurements were performed are indicated by numbers along the isotherm). Isotherm was recorded at a compression rate of 0.25 Å^2/molecule/s. (b) Schematic representation of P_{Glu}-5 unit cell. The dimensions are based on previously studied crystalline β-sheet fiber structures.[25] (c) The (0,1) Bragg peaks data (dots connected with a line for clarity), labeled with the surface pressure at the beginning of each diffraction measurement. The arrows pointing to the right and left indicate measurements acquired on compression and on expansion, respectively. (d) ln($d_{0,1}$) versus surface pressure. The points (which are labeled by the numbers that correspond to the point along the surface pressure area isotherm) were fitted with a linear equation such that (slope)$^{-1}$ of the line corresponds to the C_C compressibility value; $C_C = \partial \ln d_{0,1}/\partial\pi$ is ∼32 m/N for $\pi < 3$ mN/m and is 7.4 ± 0.6 m/N for $\pi > 3$ mN/m (see the Supporting Information for estimation of errors in ln($d_{0,1}$) and C_C).

stability of these β-sheet monolayers at the air−water interface has also been attributed to possible hydrogen-bonded arrays formed by Glu side chains,[11] which resulted in an apparent pK_a ≈ 6, higher than the ∼4.5 that is typical of the carboxyl of Glu side chain. The Pro residues positioned in the peptide termini were shown to induce the formation of 2-D ordered assemblies.[11] The GIXD pattern of the peptide Pro−Glu−(Phe−Glu)$_4$−Pro, P_{Glu}-4, exhibited a spacing of 37.4 Å, which correlated well with the previously reported distance of 6.9 Å between every second amino acid along a pleated β-sheet strand (i.e., 6.9/2 × 11 = 37.9 Å). The diffraction pattern of P_{Glu}-4 was modeled by two coexisting crystalline unit cells of similar dimensions, exhibiting two different configurations of interstrand phenyl−phenyl interactions, in addition to more subtle differences in backbone and other amino acid side chain conformations. The fact that two coexisting lattices were required to model the diffraction pattern of P_{Glu}-4 strongly implies that the peptide β-strands are structurally flexible; that is, they can assume at least these two molecular configurations and thus also switch between them. In addition, longer peptides of the same family, Pro−Glu−(Phe−Glu)$_5$−Pro (P_{Glu}-5) and Pro−Glu−(Phe−Glu)$_7$−Pro (P_{Glu}-7), exhibited spacings that were shorter than the estimated length of the peptides.[11] It was then hypothesized that the longer peptides pack in a "herringbone-like" or undulated structure such that the spacing indicated by the diffraction data reflects an oblique orientation of the strands within a ribbon. These apparent distortions could point to structural frustrations that develop in these long peptides due to the natural tendency of the strand to twist.[15,16]

Here, we present a systematic GIXD study of the peptide P_{Glu}-5 along compression and expansion surface pressure−area isotherms. We find that the β-sheet ordered monolayer structure exhibits one-dimensional quasi-reversible compressibility.

Results

The surface pressure versus mean molecular area (π−*A*) isotherm of peptide P_{Glu}-5 in Figure 1a shows the film compression and expansion. The compression isotherm starts at a low surface pressure region that extends down to the peptide limiting area per molecule (Figure 1a). At this point along the isotherm, the water interface is essentially fully covered by the peptide molecules. Further compression leads to a steep increase in surface pressure, which is followed by a collapse at $\pi \approx 25$ mN/m. The collapse state is commonly attributed to the formation of ordered or disordered multilayer structures.[17] In general, the expanding P_{Glu}-5 film (Figure 1) exhibited mean molecular areas that are smaller than during compression, suggesting the irreversible formation of molecular aggregates

(14) Smith, C. K.; Regan, L. *Science* **1995**, *270*, 980−982.

(15) Chothia, C. *J. Mol. Biol.* **1973**, *75*, 295−302.
(16) Chou, K. C.; Pottle, M.; Nemethy, G.; Ueda, Y.; Scheraga, H. A. *J. Mol. Biol.* **1982**, *162*, 89−112.
(17) Rapaport, H.; Kuzmenko, I.; Berfeld, M.; Edgar, R.; Popovits-Biro, R.; Weissbuch, I.; Lahav, M.; Leiserowitz, L. *J. Phys. Chem. B* **2000**, *104*, 1399−1428.

Table 1. Analysis of the Measured Diffraction Peaks

π (mN/m)	mma[a] (Å²/molecule)	q_{xy} (Å^{-1})	d[b] (Å)	fwhm$_{xy}$[c] (Å^{-1})	L_{xy}[d] (Å)	I_{max}[e] (au)	q_z[f] (Å^{-1})	fwhm$_z$ (Å^{-1})	h_z (Å)
				(0,1)					
1.4	200	0.1365	46.0	0.0251	225	4740	0.203	0.454	12.44
6.7	187	0.1474	42.6	0.0231	244	4563	0.300	0.370	15.27
17.1	169	0.1613	38.9	0.0223	254	4480	0.375	0.310	18.21
23.0	156	0.1694	37.1	0.0227	249	3830	0.380	0.289	19.59
27.6	139	0.1748	35.9	0.0224	253	3448	0.369	0.269	21.01
27.1	126	0.1752	35.8	0.0203	278	3250	0.374	0.354	15.98
29.7	93	no peak							
16.4	140	0.1585	39.6	0.0192	294	3091	0.376	0.538	10.50
11.5	154	0.1565	40.1	0.0208	272	3151	0.310	0.498	11.34
0.0	201	0.1305	48.1	0.0251	225	2620	0.144	0.437	12.93
				(2,0)[g]					
1.3	200	1.3178	4.77	0.0483	117	9418	0.166	0.404	13.99
6.4	187	1.3134	4.78	0.0697	81	11 581	0.037	0.652	8.67
16.7	169	1.3219	4.75	0.0528	107	8878	0.157	0.330	17.13
23.5	156	1.3162	4.77	0.0821	69	6335	0.128	0.341	16.56

[a] Mean molecular area, measured along the isotherm. [b] The spacing corresponding to q_{xy}, $d = 2\pi/q_{xy}$. [c] The full width half-maximum of the Bragg peak at q_{xy}. [d] The coherence length of the ordered domain $L_{xy} = 0.9 \times 2\pi/\text{fwhm}_{xy}$. [e] The maximum intensity of the Bragg peak. [f] q_z, fwhm$_z$, and h_z are the Bragg rod position maxima, full width half-maxima, and height, respectively. The height is estimated according to $h_z = 0.9 \times 2\pi/\text{fwhm}_z$. The full $I(q_z)$ pattern of the Bragg rod data is provided in Figure 2. [g] The (2,0) data were collected on compression. The small deviations in π values from the corresponding (0,1) data are probably due to film relaxation.

along the collapse region of the isotherm. The GIXD measurements described below provide structural insights on P_{Glu}-5 film undergoing the compression−expansion cycle.

GIXD measurements of P_{Glu}-5, performed along the compression−expansion cycle isotherm, yielded, in general, two distinct Bragg peaks: one that corresponds to the β-sheet hydrogen-bond direction and the other related to ordered β-strands, along the backbone axes (Figure 1b). Table 1 summarizes the analysis of the measured diffraction peaks. The first measurement performed along the compression isotherm, at $\pi = 1.4$, showed the two typical diffraction peaks, (0,1) at $q_{xy} = 0.1365$ Å^{-1}, and (2,0) at $q_{xy} = 1.3178$ Å^{-1}, that correspond to spacings $d_{0,1} = 46.0$ Å and $d_{2,0} = 4.8$ Å, respectively. These two Bragg peaks indicate the formation of a 2-D ordered lattice, with lattice vectors of $a = 9.6$ Å and $b = 46.0$ Å (cf., Figure 1b). The lattice vector a is set to double the observed spacing because neighboring strands, along the a direction, are oriented in the antiparallel mode.[11] A definite unit cell cannot be determined on the basis of two Bragg peaks only in the 2-D powder pattern. Nevertheless, it is reasonable to assume that the unit cell is characterized by a γ angle of ∼90°, as the long spacing, 46 Å, is close to the estimated length of a 13-residue peptide in the β-pleated conformation, projected on the water interface, that is, $\sim 6.9/2 \times 13 = 44.8$ Å (see Figure 1b and legend). Hence, the P_{Glu}-5 lattice at $\pi = 1.4$ mN/m may be described by the unit cell $a = 9.5$, $b = 46.0$ Å, $\gamma \approx 90°$ with an area per molecule of $(9.5 \times 46.0)/2 = 218.5$ Å^2 corresponding to $218.5/13 = 16.8$ Å^2 area per residue.

Interestingly, the P_{Glu}-5 (0,1) Bragg peak that corresponds to the spacing along the β-strand backbone direction was found to shift to higher q_{xy} values (smaller spacings) on increase of the applied surface pressure (Figure 1c and Table 1). For example, at $\pi = 1.4$ mN/m, the detected (0,1) spacing is $d_{0,1} = 46$ Å and at $\pi = 27.1$ mN/m, $d_{0,1} = 35.8$ Å, a reduction by 22% in length. Upon further compression to $\pi = 29.7$ mN/m, the (0,1) Bragg peak could no longer be detected. Upon expansion of the same film and release of the applied surface pressure, the Bragg peak reappeared at q_{xy} versus π values similar to those obtained along the compression (Table 1). Upon expansion of the film, the longest (0,1) detected spacing was 48.1 Å, larger than the 46 Å, obtained along the compression, at $\pi = 1.4$ mN/m. This difference of ∼2 Å may be related to the backbone flexibility, or to changes in the interactions of the peptide termini, affecting the gaps between neighboring ribbons. The fact that along the film expansion the (0,1) Bragg peaks reappear at q_{xy} values similar to those obtained along the compression isotherm implies that under applied pressure the crystalline β-sheet monolayer film deforms elastically and approximately reversibly. Nevertheless, Figure 1c depicts a continuous decrease in the intensity of the (0,1) Bragg peak all along the compression and the expansion isotherm, indicating a destruction of the ordered peptide domains, which occurs probably due to shear stresses and interfacial forces resulting from film compression and expansion as well as from beam damage caused by the repeating X-ray scans. Moreover, the shape of the Bragg rods (the out-of-plane diffraction, see Figures 2a and 3 and Table 1) indicates a shift of the maxima of the (0,1) rods toward higher q_z values on increase of surface pressure, that is, from $q_z = 0.2$ Å^{-1} at $\pi = 1.4$ mN/m to $q_z \approx 0.37-0.38$ Å^{-1} at $\pi \geq 17$ mN/m with concomitant increase in the estimated thickness (h_z, see Table 1) of the ordered film. These changes in Bragg rod shape suggest an out-of-plane bending of the β-strands backbone in reaction to the increase in surface pressure. The (2,0) Bragg peaks that correspond to the interstrand spacing, that is, along a, the hydrogen-bonds direction, maintained almost the same q_{xy} position (spacing $d_{2,0} = 4.75-4.78$ Å) as well as $I(q_z)$ Bragg rod shapes, throughout the compression and expansion measurements (Figure 2b and Table 1); thus the compressibility in this direction is ∼0, within experimental error. Similar to the trend observed in the (0,1) data, there is also a general decrease in the (2,0) Bragg peak intensities on compression.

The crystallographic unit cell parameters together with the mean area per molecule of the compression isotherm and the applied surface pressure allow the evaluation of film compressibility. The macroscopic 2-D compressibility, C_M, is extracted from the surface pressure−area isotherms, and the compressibility of the crystalline domain, C_C, is based on the diffraction

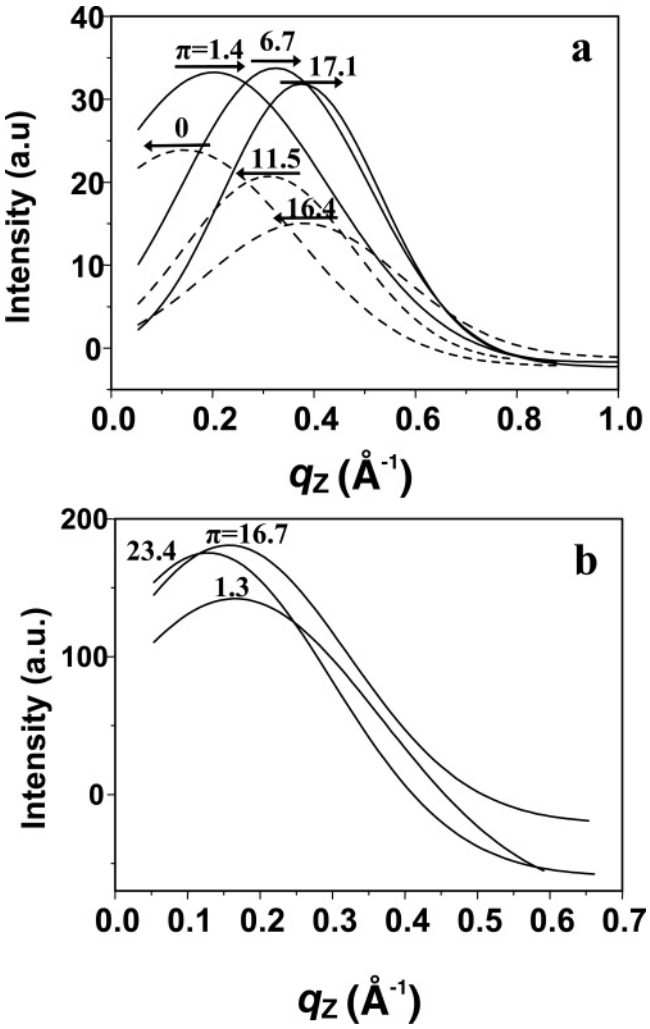

Figure 2. A few of the observed GIXD Bragg rod patterns of P_{Glu}-5 monolayer at various surface pressures (labeled curves): (a) (0,1), (b) (2,0). The Bragg rods data presented in Table 1 are based on the analysis of these curves. The Bragg rods are represented by Gaussian curves fitted to the experimental data along compression (−) and expansions (− − −); these figures with the experimental data are provided in the Supporting Information.

data. The compressibility of a Langmuir film, in general, is defined as:

$$C = -(\partial \ln A/d\pi)_T \qquad (1)$$

where A is the peptide area per molecule. The compressibility of the crystalline β-sheet, C_C, may be calculated from the two observed Bragg peaks, assuming (cf., above) that $\gamma \equiv 90°$. In the present case, as described above, only the (0,1) spacing changes and the (2,0) remains constant along the compression, hence

$$C_C = -(\partial \ln d_{0,1}/\partial\pi)_T - (\partial \ln d_{2,0}/\partial\pi)_T \approx -(\partial \ln d_{0,1}/\partial\pi)_T \qquad (2)$$

The $\ln(d_{0,1})$ values, along both the compression and the expansion isotherms, follow two characteristic lines with different slopes (Figure 1d). At surface pressures higher than $\pi \approx 3$mN/m, the curve slope indicates $C_C = 7.4 \pm 0.6$ m/N. A several times larger value, $C_C = 32$ m/N, was estimated for the low surface pressure ($<\sim$3 mN/m) region of the isotherm (Figure 1a and d). Noteworthy, although the data plotted in Figure 1d could be reasonably divided into two regions characterized by different compressibility values, the reliability of $C_C = 32$ m/N, attributed to the expanded film, is much smaller as compared to that of the compressed film $C_C = 7.4 \pm 0.6$ m/N. The former is based on only two data points (Figure 1a and d), one obtained along compression and the other along film expansion. In evaluating C_M, the macroscopic compressibility, A in eq 1, corresponds to the mean area per molecule (Figure 1a). The surface pressure−area isotherm represents the mechanical properties of the Langmuir film, taking into account both the crystalline and the amorphous parts. The C_M compressibility is found from the slope of the compression isotherm that is represented as π versus $\ln(A)$ (figure provided in the Supporting Information). The compression isotherm of P_{Glu}-5 may be described by two characteristic values of compressibility. Along the compression isotherm following the onset in surface pressure at the limiting area per molecule ($\sim$200 Å^2) and up to the collapse at surface pressure of $\sim$25 mN/m (mean area per molecule $\sim$150 Å^2), the film exhibits a compressibility of $C_M = 11.3$ m/N that is quite similar to the $C_C = 7.4 \pm 0.6$ m/N of the crystalline β-sheet structure. Along the inclined plateau where the film presumably collapses into multilayer structures, the compressibility is an order of magnitude larger, $C_M = 112$ m/N.

Summary and Discussion

In summary, this study has provided experimental evidence of β-sheet elastic-like behavior that was detected by grazing incidence X-ray diffraction measurements, performed along surface pressure−area isotherms. The results reveal two characteristic compressibility regions for crystalline P_{Glu}-5 assemblies below and above $\pi \sim 3$ mN/m, respectively. It is

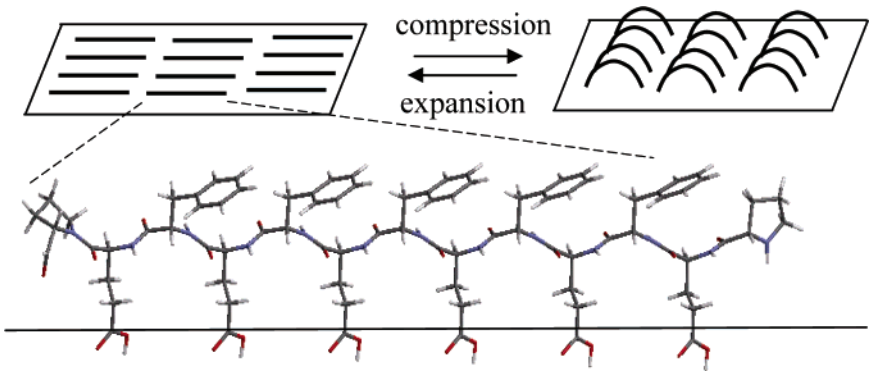

Figure 3. Schematic representation of the suggested conformational changes the β-strands backbones undergo on compression and expansion of the film.

reasonable to assume that the crudely estimated higher compressibility, $C_C = 32$ m/N, obtained at low surface pressure, is mostly dominated by inter-ribbon adjustments induced by the decrease in the film area. At higher surface pressures, the lower compressibility, $C_C = 7.4 \pm 0.6$ m/N, arises from considerable conformational deformation that is necessarily affecting the shape of the peptide backbone. The P_{Glu}-5 Langmuir isotherm exhibits a macroscopic compressibility $C_M = 11.3$ m/N that is close to the compressibility attributed to the peptide backbones in the crystalline structure. This similarity is explained by the fact that beyond the limiting area per molecule where peptides are closely packed, the compression affects the peptide backbone conformation both in the crystalline domains and in the nonordered domains, and to a less extent the lateral arrangement of the molecules on the surface.

Preliminary structure factor calculations, in combination with molecular modeling, suggest that, upon compression, the peptides within the ordered β-sheet domains bend out of the water interface. This hypothesis is supported by the differences in the projected area occupied by Phe versus that of Glu. It is reasonable to assume that the peptide backbone buckles such that the Glu side chains get closer to each other and the distance between the hydrophobic Phe side chains becomes longer such that overall the peptide backbone appears bent out of the water interface. According to our experiments, on increase in surface pressure that is equivalent in three dimensions to hydrostatic pressure, the backbone axis yields before any deformation along the β-sheet interstrand hydrogen-bond direction.

Conformational flexibility of β-strands and sheet structures manifests in diverse coiled, twisted, bent, and sheared-sheet configurations in globular proteins.[18−20] Wang and Small used an oil-drop tensiometer to study the surface tension and elastic modulus (that is, the inverse of the P_{Glu}-5 macroscopic compressibility value measured here) of consensus sequences derived from apolipoprotein B.[21] There is a good match between the highest elastic modulus, that is, the lowest compressibility value measured by Wang and Small, for apolipoprotein B, ~7−11 m/N, and the $C_C = 7.4 \pm 0.6$ m/N and $C_M = 11.3$ m/N compressibility values found in this study for P_{Glu}-5 monolayer. Interestingly, on the basis of their measurements, the authors suggested that β-sheet film complies elastically to a reduction of up to 25% in film area. The results presented here provide direct X-ray diffraction evidence for the β-sheet elastic deformation. According to our results, the P_{Glu}-5 crystalline β-sheet domains may be compressed by ~37% (from 200 to 126 Å^2/molecule, Table 1).

Noteworthy, compressibility has also been detected in ordered helical assemblies of alamethicin. On the basis of the data reported by Ionov et al.,[22] a compressibility of ~2.6 m/N along the axes of the helices may be estimated. Nevertheless, more diffraction measurements are required to elucidate the conformational changes that characterize the helical compression.

The compressibility of Langmuir films composed of long chain amphiphilic compounds has been studied both theoretically[23] and experimentally by GIXD.[24] The largest compressibilities (10 m/N) were observed for phases in which the long chains are tilted away from the normal of the water interface. These were found to be independent of chain length, and thus were attributed to reorganization of headgroup hydrogen-bond networks. The lowest compressibility values, observed in the solid, untilted phase, were found to be similar in value to those of crystalline polymers associated with rearrangements of methyl groups in the crystal state.[24]

It is reasonable to assume that the β-sheet compressibility depends on the peptide sequence and on the packing of the strands. Therefore, more measurements are currently underway to assess the compressibility of various β-sheet monolayer systems. We believe that the structural and mechanical insights provided here will contribute to a better understanding of β-sheet assemblies in the context of designed biomaterials, in natural proteins and amyloid fibers.

Acknowledgment. This work was supported by the Israel Science Foundation. K.K. thanks the Carlsberg Foundation and the DanSync Programme of the Danish Natural Science Research Council. GIXD studies at beam-line BW1, Hasylab, DESY, were supported by the European Community-Research Infrastructure Action under the FP6 "Structuring the European Research Area" Programme (through the Integrated Infrastructure Initiative "Integrating Activity on Synchrotron and Free Electron Laser Science").

Supporting Information Available: Experimental section. Full P_{Glu}-5 isotherm obtained during GIXD measurements and comments thereon. Figure of the Bragg rod data points of the (0,1) and (2,0) peaks and the π versus ln(A) figure of P_{Glu}-5 with the C_M compressibility values. Error calculations for ln($d_{0,1}$) and C_C ($\pi > 3$ mN/m). This material is available free of charge via the Internet at http://pubs.acs.org.

JA062363Q

(18) Salemme, F. R.; Weatherford, D. W. *J. Mol. Biol.* **1981**, *146*, 119−141.
(19) Ho, B. K.; Curmi, P. M. G. *J. Mol. Biol.* **2002**, *317*, 291−308.
(20) Emberly, E. G.; Mukhopadhyay, R.; Tang, C.; Wingreen, N. S. *Proteins: Struct., Funct., Bioinf.* **2004**, *55*, 91−98.
(21) Wang, L.; Small, D. M. *J. Lipid Res.* **2004**, *45*, 1704−1715.
(22) Ionov, R.; El-Abed, A.; Angelova, A.; Goldmann, M.; Peretti, P. *Biophys. J.* **2000**, *78*, 3026−3035.
(23) Hu, J.-G.; Granek, R. *J. Phys. II France* **1996**, *6*, 999−1022.
(24) Fradin, C.; Dalliant, J.; Braslau, A.; Luzet, D.; Alba, M.; Goldman, M. *Eur. Phys. J. B* **1998**, *1*, 57−69.
(25) Krejchi, M. T.; Atkins, E. D. T.; Waddon, A. J.; Fournier, M. J.; Mason, T. L.; Tirrell, D. A. *Science* **1994**, *265*, 1427−1432.